Journal of Applied Mathematics and Physics, 2023, 11, 2997-3008
https://www.scirp.org/journal/jamp
ISSN Online: 2327-4379
ISSN Print: 2327-4352

Numerical Simulation for the Efficiency of the Produced Terahertz Radiation by Two Femtosecond Laser Pulses: Above-Threshold-Ionization

Abdelrahman Mahdy

Physics Department, College of Science, Jazan University, Jazan 45142, Saudi Arabia
Email: amahdy@jazanu.edu.sa

How to cite this paper: Mahdy, A. (2023) Numerical Simulation for the Efficiency of the Produced Terahertz Radiation by Two Femtosecond Laser Pulses: Above-Threshold-Ionization. *Journal of Applied Mathematics and Physics*, **11**, 2997-3008.
https://doi.org/10.4236/jamp.2023.1110198

Received: September 29, 2023
Accepted: October 23, 2023
Published: October 26, 2023

Abstract

The tunneling ionization (TI) is the most dominated ionization process in the production of terahertz radiation by two femtosecond lasers, although its validity above the ionization threshold of some gases is uncertain. In the present research, we employ a 1D fluid code to simulate the efficiency of the produced terahertz radiation by two femtosecond laser beams in air plasma. Two ionization models in the context of the TI process which are the Ammosov-Delone-Krainov (ADK) for noble gases and its developed molecular ADK (MO-ADK) model for molecular gases are intrinsically used to conduct this study. The main target of the present research is to examine the validity of these models Above-Threshold-Ionization (ATI) of these gases. For this purpose, we simulated the ionization rate and the power spectrum of the produced radiation, in addition we numerically evaluated the efficiency of the produced radiation as function of the input beams intensity at particular energy fraction factor, relative phase and initial pulse duration of these beams. These calculations conducted for a selected noble gas at varying energy levels and a chosen molecular air plasma gas at different quantum numbers. Numerical results near and above the ionization threshold of the selected gases have clarified that the ADK and MO-ADK model are successful valid to study the efficiency of the produced THz radiation at low energy levels and small quantum numbers of the selected gases, meanwhile, with any further increase in the energy level and the quantum number values of these gases, both of the ADK and MO-ADK are failed to correctly analyze the efficiency process and estimate its fundamental parameters.

Keywords

Terahertz Radiation Production, Femtosecond Laser, Computational Physics

1. Introduction

Because of its non-destructive and non-contact properties, and label-free optical method, the terahertz radiation has a growing attention in security inspection [1], biological imaging and spectroscopy [2], biomedicine [3], THz communication [4] [5], and industry [6] [7]. In air plasma, the filamentaion of two-color femtosecond (fs) laser beams is the fundamental mechanism of the terahertz radiation production. In this mechanism, a fundamental laser pulse (FH) and its corresponding second harmonic (SH) are applied to excite the terahertz wave, two theories are govern the production under this two fs lasers approach: the Four-Wave Mixing rectification (FWM) [8] and the Photo-current theory (PC) [9].

In both of FWM and PC theory, the tunneling ionization [10] is the dominated ionization event. In this process, a number of electrons are released from the atomic barrier formed by the Coulomb potential coupled with strong laser electric field, these removed electrons are accumulated along asymmetric filed induced by the two fs beams that accelerate the released electrons to induce a current which oscillates to a low-frequency current responsible for THz wave emission. In air plasma, the mostly and widely used tunneling ionization models are Ammosov-Delone-Krainov (ADK) [11] and the molecular-ADK (MO-ADK) model [12]. Both models have a good agreement with the experiments in noble gases and small molecules [13] [14] [15]. The ADK model is approved on the noble gases, with an additional implementation for the structure-less atomic like molecules such as H_2, while the MO-ADK model is mainly applied to calculate the ionization from molecules [12]. A number of researches have investigated the THz emission via the interaction of laser pulse with noble gases [16] [17] (He, Ne, Ar, Kr, and Xe) and molecular gases [18] [19] [20] [21] [22] (H_2, H_2O, N_2 and O_2) based on the ADK and its developed MO-ADK model. It has been found in some of these researches that the ADK model overestimates the ionization rate of atoms in the over-the-barrier ionization (OBI) regime [23] [24] [25] and fails to anticipate the correct ionization probability in the multi-photon ionization regime. With respect to the MO-ADK model, although it has also been developed to involve on the THz radiation generation [26] and to study the ionization of the H_2O molecule in the OBI regime [24], the MO-ADK unsuccessfully estimates the accurate ionization rates of ion-electron interactions [27] and when the above threshold ionization (ATI) is required. Although extensions have been developed for static ATI [24], the MO-ADK is remained unable to predict the ionization suppression of Cl_2 in comparison to Xe. Therefore, an elaborated analysis on the interaction of the fs laser with noble and molecular air plasm gases for the production of THz radiation is required to examine of the validity of the ADK and its developed MO-ADK model near and above the threshold ionization of these gases.

In this article, we study the production of the terahertz radiation by the filamentaion of two femtosecond laser beams in air plasma. In particular, using a

1D fluid code, we numerically simulate the efficiency of the produced radiation in noble gases using the standard Ammosov-Delone-Krainov (ADK) ionization rate formula and in molecular gases using the developed molecular-ADK (MO-ADK) formula. Our main objective is to examine the validity of the two formulas above the threshold ionization (ATI) at varying energy levels of the noble gases and different quantum numbers of the air molecules. The article is organized as follow: in Section 2, we present the numerical code by listing its basic equations and describing the numerical solution method. In Section 3, we present numerical simulation for the ionization rate and power spectrum of the produced radiation, beside, at particular energy factor, relative phase and initial pulse of the applied beams, we evaluate the conversion efficiency of the produced radiation as function of the input beams intensity at varying energy levels of a selected noble gas and different quantum numbers of a given air molecule.

2. Numerical Algorithm

In the numerical code employed to simulate the efficiency of the produced THz radiation by two femtosecond laser beams in air plasma, the propagation of the beams is describing by the following 1D Maxwell's equation:

$$\nabla \times \boldsymbol{E} = -\frac{\partial \boldsymbol{B}}{\partial t} \tag{1}$$

$$\nabla \times \boldsymbol{B} = \mu_0 \boldsymbol{J} + \mu_0 \varepsilon_0 \frac{\partial \boldsymbol{E}}{\partial t}.$$

E and B are electric and magnetic field, respectively, J is the charge density, ε_0 is the permittivity and μ_0 is the permeability of free space. The electrons dynamics is followed by the momentum equation

$$\frac{\partial \boldsymbol{J}}{\partial t} + v_c \boldsymbol{J} = \frac{e^2}{m} N_e \boldsymbol{E}. \tag{2}$$

where e and m are the electron charge and mass respectively, N_e initial gas density, v_c electron-neutron collision.

For the electrons production and ionization, for the noble gases the standard the Ammosov-Delone-Krainov (ADK) [11] [28] formula is used.

$$W_i^Z(t) = 4\omega_{at}\left(r_H^i\right)^{5/2}\left(\frac{E_{at}}{\left|E(r,t)\right|}\right)\exp\left(-\frac{2\left(r_h^i\right)^{3/2} E_{at}}{3\left|E(r,t)\right|}\right). \tag{3}$$

In above formula $\omega_{at} = mq^2 / \left(4\pi\varepsilon_0^2\right)\hbar^3 = 4.134\times10^{16}\ \text{s}^{-1}$ is the atomic frequency, $E_{at} = m^2 q^5 / \left(4\pi\varepsilon_0^3\right)\hbar^4 = 5.14\times10^9\ \text{V/cm}$ is the atomic unit of the electric field, and E_L is the electric field of the applied fs beams. $r_H^i = E_i^Z / E_H$, where E_i^Z is the ionization energy of the gas of Z atomic number, i is the ionization-energy order of this gas, and E_H is the ionization energy of the hydrogen. With respect to the molecular gas, the following MO-ADK ionization rate of a linear diatomic molecule of a slowly varying field is considered [29]

$$W_{\text{MO-ADK}}(\varepsilon) = \frac{B^2(m)}{2^{|m|}|m|!}\frac{1}{\kappa^{2Z_c/\kappa-1}}\left(\frac{2\kappa^3}{\varepsilon}\right)^{(2Z_c/\kappa)-|m|-1} \mathrm{e}^{-\kappa^3/3\varepsilon}. \tag{4}$$

Z_c being the effective Coulomb charge, $\kappa = \sqrt{2I_p}$ to be the residual charge of the molecular system, and I_p being the ionization potential for the given valence orbital, m being the magnetic quantum number, and the function $B(m) = \sum_{\ell} C_{\ell} Q(l,m)$, where

$$Q(l,m) = (-1)^m \sqrt{\frac{(2\ell+1)(\ell+|m|)!}{2(\ell-|m|)!}}$$

The finite-difference time-domain (FDTD) method [30] [31] [32] [33] is applied to solve our basic equations; Maxwell's equations coupled with the monument equation and the ionization rate formulas. The FDTD that calculates E and B in space and time domain is used because of its unique properties to present a direct solution in time domain and for its good estimation to E and B near the boundaries. To reduce the computational time in our simulation, absorbed boundaries are assumed.

In our simulation the following initial laser beam profile $E_L(t)$ is given:

$$E_L(t) = E_m\left(\sqrt{1-\zeta}\sin(\omega_0 t)\mathrm{e}^{-\frac{t^2}{2\tau_0^2}} + \zeta\sin(2\omega_0 t + \phi)\mathrm{e}^{-\frac{t^2}{\tau_0^2}}\right). \quad (5)$$

where $E_m = \sqrt{2I_0/\varepsilon_0 c}$ is the amplitude, $\omega_0 = 2\pi c/\lambda$ ($\lambda = 800\ \text{nm}$), I_0 is the initial input intensity, ζ is the energy fraction factor, ϕ is the relative phase between the two beams, and $\tau_0 = 40\ \text{fs}$ is the initial pulse duration. The plasma sample in our simulation is semi-bounded plasma with a width $d = 90\ \mu\text{m}$.

3. Simulation Results

In order to analyze the efficiency of THz radiation produced in the frame of the standard ADK and its developed MO-ADK model, a noble and a molecular air gas element have to designated at first. In that context, the Argon (Ar) is elected among the noble gases and the molecular N_2 is chosen among the air molecules. The selected noble and molecular gas are highly regraded and popular elements on the air structure, but the mostly emphasized reason of this selection is the multi energy levels n of Ar and the high quantum number ℓ of N_2, which will give us a good deal of opportunities to analyze the efficiency of the produced THz radiation for varying energy levels and different quantum numbers. The ionization energies of the Ar are listed in **Table 1**, and the values of C_ℓ for N_2 derived for MO-ADK [12] are given in **Table 2**.

Table 1. Ionization energy (eV) of Argon (Ar).

Ionization order	1	2	3	4
Ionization energy	15.7596117	27.62967	40.735	59.58

Table 2. Values for C_ℓ.

Species	C_0	C_1	C_2	C_3	C_4
N_2	2.02	-	0.78	-	0.04

After we have designated the noble gas Ar and the air molecule N_2 for our analysis, it is vitally important to note before starting this analysis that the initial beams profile given in Equation (5) is determined based on the initial input intensity I0, the energy fraction factor ζ, and the relative phase ϕ values. The initial I0 value depends on the selected n of Ar and on the given ℓ of N_2 ionization energy, while the energy fraction ζ and the relative phase ϕ have to be optimized.

To optimize the energy fraction factor ζ and the relative phase ϕ, we simulate in **Figure 1** the ionization rate (n_e/n_0) as function of possible ζ and ϕ range. The ionization rate based on the ADK model is given on left and the one based on the MO-ADK formula is shown on right. For ADK, the energy level $n=1$ and its above ionization intensity value $I_0 \approx 1.4\times10^{14}\ \mathrm{W/cm^2}$ are given, and for the MO-ADK, the quantum number $l=0$ and its above ionization intensity $I_0 \approx 2.5\times10^{14}\ \mathrm{W/cm^2}$ are considered. As display on both ionization rates, the maximum ionization rate is demonstrated for the two models at approximately $\zeta=0.5$ and $\phi=\pi/2$. Truthfully, this obtained fraction energy value is physical expected, as in the interactions of two fs beams at equal input energy, *i.e*, $\zeta=0.5$, numerous of effects that reduce the energy delivering to medium; such energy exchange and the associated modulation instabilities, are halted to enhance the ionization process. With regard to the optimized relative phase, as matter of fact this value is also anticipated, as it has been introduced in previous researches $\phi=\mathrm{pi}/2$ the relative phase where the maximum terahertz efficiency is achieved [34]. On the other hand, what is astonishing in the results exposed in **Figure 1** is that the optimized ζ and ϕ are the same for both of the ADK and MO-ADK model.

Optimizing the energy factor and the relative phase factor is not the only we can attain from the ionization rate image presented in **Figure 1**, but also examining the performance and the validity of the ADK and MO-ADK model above-threshold ionization (ATI). As it is clearly shown in **Figure 1**, the ionization rate is stable and continuous over the given ζ and ϕ range, obtaining

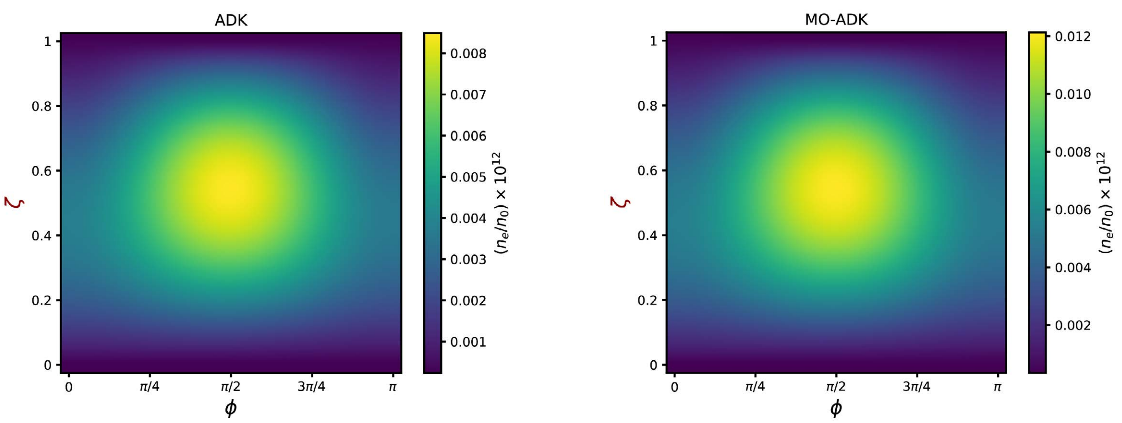

Figure 1. The ionization rate under the ADK (left) formula at $I=1.4\times10^{14}\ \mathrm{W/cm^2}$ and $n=1$ and the MO-ADK (right) at $I=2.5\times10^{14}\ \mathrm{W/cm^2}$ and $\ell=0$.

such favorable ionization rate features affirms the successful performance and validity of the ADK and MO-ADK model Above-threshold ionization (ATI) at the given n and ℓ value.

The ionization rate shown in Figure 1 is not the only approach to examine validity of our ADK and MO-ADK models, the power spectrum of the produced THz radiation is another admitted alternative for this examination. In this regards, we present in Figure 2 the power spectrum μ_{THz} of the produced THz radiation as function of the energy fraction factor ζ and the relative phase ϕ of the applied two fs laser beams. This result is presented at higher energy level and quantum number, which are $n=2$ and $\ell=2$, thus $I_0=1.8\times10^{14}\ \text{W/cm}^2$ and $I_0=3.1\times10^{14}\ \text{W/cm}^2$ are given as ATI value for ADK and MO-ADK model, respectively. As depicted in Figure 2, the maximum power is demonstrated at $\zeta=0.4\text{-}0.8$ and $\phi=\pi/8\text{-}\pi/4$ for the ADK and at $\zeta=0.6\text{-}0.8$ and $\phi=0\text{-}\pi/4$ for the MO-ADK model. Regardless of the optimized ζ and ϕ value that are emerged differently from the values obtained in Figure 1, the continuous and stable power spectrum is clearly observed even at such higher n and ℓ, which confirms the extended validity of our ADK and MO-ADK models to such energy level and quantum number value.

Although, we have presented in Figure 1 and Figure 2 a preliminary examination for the validity of the ADK and the MO-ADK model ATI for selected noble and molecular gas at particular energy level n and quantum number ℓ value, it is necessary to bear in mind that evaluating the conversion efficiency η_{THz} of the produced THz as function of the input beams intensity ATI is the pre-eminent and the well-acknowledge procedure to examine the validity of our ADK and MO-ADK models. Upon that, the main task of the simulation presented in Figure 1 and Figure 2 will be remained to optimize the suitable energy fraction factor ζ and relative phase value at the given n and ℓ value.

Based on above considerations, in Figure 3 we present the conversion efficiency η_{THz} of the produced THz radiation as function of the input intensity of

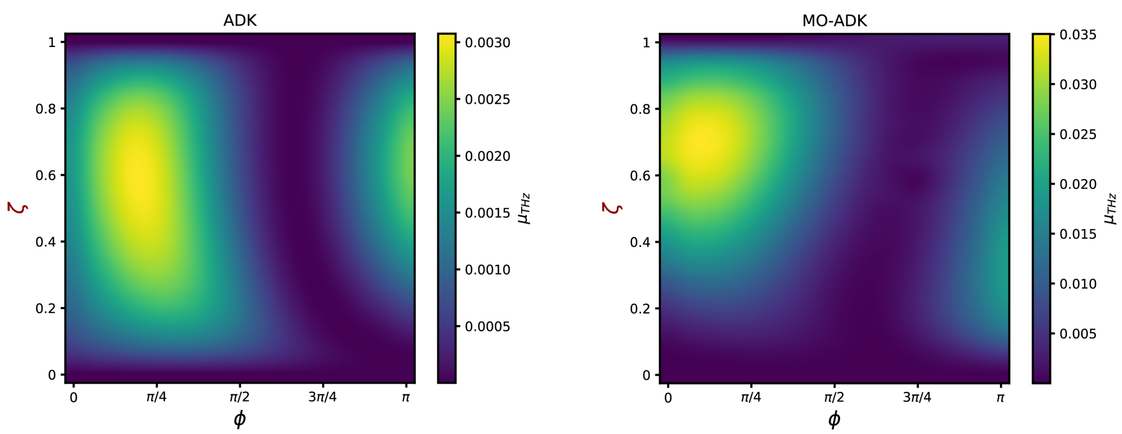

Figure 2. The power spectrum of the produced THz radiation The ionization rate under the ADK (left) formula at $I=1.8\times10^{14}\ \text{W/cm}^2$ and $n=2$ and the MO-ADK (right) at $I=3.1\times10^{14}\ \text{W/cm}^2$ and $\ell=2$.

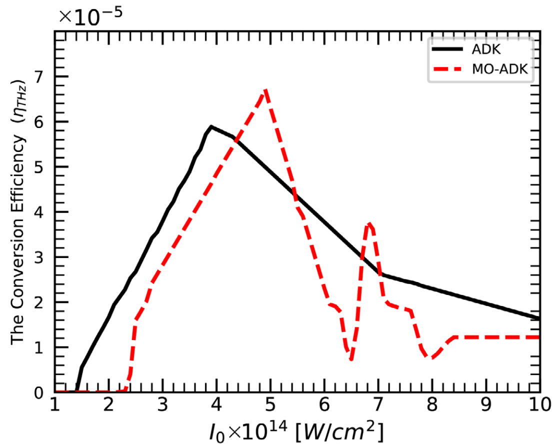

Figure 3. The conversion efficiency η_{THz} of the produced THz radiation as function of the input beams intensity for Ar at $n=1$ under ADK and N_2 at $\ell=0$ under the MO-ADK model.

the two femtosecond laser beams above the threshold ionization of the Ar noble gas at $n=1$ and N_2 molecule at $\ell=0$, the optimized $\zeta=0.5$ and $\phi=\phi/2$ are considered in this figure. As detailed in **Figure 1**, the basic precesses associated with the efficiency behavior as function of the input beams intensity are clearly demonstrated. First, the near/above ionization threshold intensity where the ionization process of the noble and molecular gas element starts, which as measured $I_0=1.4\times10^{14}\ \text{W/cm}^2$ for ADK and $I_0=2.5\times10^{14}\ \text{W/cm}^2$ for the MO-ADK. Second, the linear increment of the efficiency with increasing the input beams intensity shortly after the ionization establishing. Third, the maximum ionization intensity where the elements are completely ionized, which as evaluated in the figure $I_0\approx3.8\times10^{14}\ \text{W/cm}^2$ for ADK and $I_0\approx5\times10^{14}\ \text{W/cm}^2$ for the MO-ADK. Lastly, the efficiency decaying after the complete ionization of the designated gases, which is smoothly decaying for the Ar under the ADK and abruptly decaying for N_2 under the MO-ADK model. In addition to the basic processes associated with the efficiency behavior, the fundamental parameters of these processes are accurately measured in **Figure 4**. As the near/above ionization threshold intensity values for the two elements are nearby to the previously reported values [31], in addition, the maximum ionization intensities for the designated gases are within the acceptable range, moreover the higher efficiency value for the MO-ADK than the ADK which is usually behaved.

In **Figure 4** we present the conversion efficiency η_{THz} of the produced THz radiation as function of the input beams intensity above the threshold ionization of the Ar noble gas at $n=2$ and N_2 molecular gas at $\ell=2$, the optimized $\zeta=0.5$ and $\phi=\phi/8$ are given in this figure In this figure, the basic processes that get together with the efficiency behavior such as the near/above ionization threshold intensity, the linear increment of the efficiency with increasing the input beams intensity, the maximum ionization intensity, and the efficiency

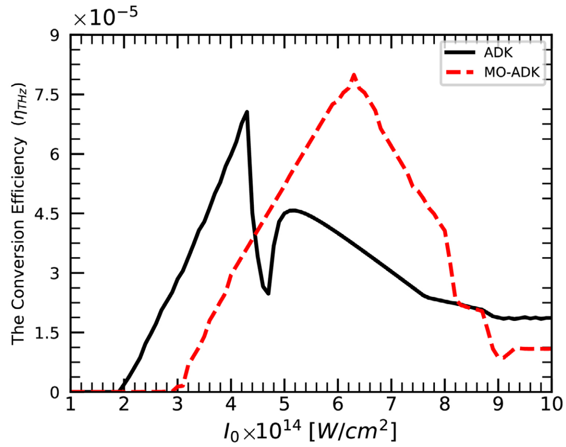

Figure 4. The conversion efficiency η_{THz} of the produced THz radiation as function of the input beams intensity for Ar at $n=2$ under ADK and N_2 at $\ell=2$ under the MO-ADK model.

decaying are clearly determined. Moreover in **Figure 4**, the fundamental parameters of these processes for the given noble and molecular gas, as the threshold ionization intensity $I_0 \approx 2\times10^{14}\ \text{W/cm}^2$ for ADK and $I_0 \approx 3\times10^{14}\ \text{W/cm}^2$ for the MO-ADK are approximately at the standard values [31] [35], and the maximum ionization intensity $I_0 \approx 4\times10^{14}\ \text{W/cm}^2$ for ADK and $I_0 \approx 6.5\times10^{14}\ \text{W/cm}^2$ for the MO-ADK are around the acceptable range.

In **Figure 5** we present the conversion efficiency η_{THz} of the produced THz radiation as function of the intensity of the two fs beams above the threshold ionization of the Ar noble gas at $n=3$ and N_2 molecular gas at $\ell=4$, the optimized $\zeta=0.5$ and $\phi=\phi/2$ are considered in this figure As demonstrated in **Figure 5**, although the near/above ionization threshold intensities are determined, its values are inaccurately measured, because these values are the same values measured in **Figure 4** at the lower n and ℓ order. Even though the efficiency is linearly incremented with the input beams intensity, this efficiency is in incorrectly estimated, as seen at the maximum ionization intensity this efficiency for the two different gas elements are approximately equal. Lastly, the decaying behavior is un-precisely conducted, as its is saturated without any decaying for the two models after the ionization completion.

4. Conclusion

We have numerically simulated the efficiency of terahertz radiation produced by two femtosecond laser beams in noble and molecular air plasma gas. The standard Ammosov-Delone-Krainov (ADK) model for the noble gases and the developed molecular ADK (MO-ADK) model for molecular gases are used in this study. We have targeted to examine the validity of these models above the threshold ionization of these gases, in this regard, by means of 1D fluid code, at a particular energy fraction factor ζ, relative phase ϕ, and pulse duration τ_0

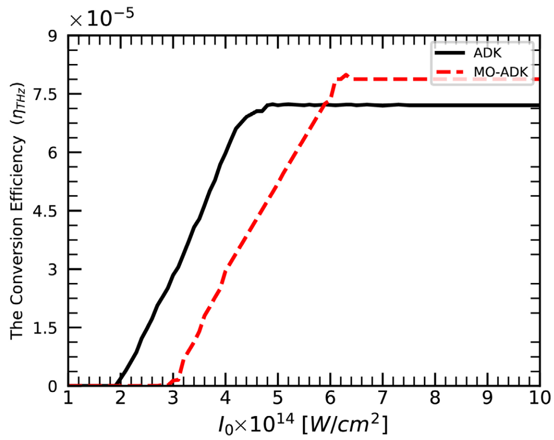

Figure 5. The conversion efficiency η_{THz} of the produced THz radiation as function of the input beams intensity for Ar at $n=3$ under ADK and N_2 at $\ell=4$ under the MO-ADK model.

of the applied beams, we have simulated the ionization rate and the power spectrum of the produced radiation. As well we have evaluated the conversion efficiency of this radiation as the function of the input intensity of these beams for varying energy levels of a selected noble gas and different quantum numbers of a chosen air molecule. Numerical results have illustrated that at low energy levels n of Ar noble gas and small quantum numbers ℓ of N_2 molecule, the ADK and the MO-ADK model are successfully valid to investigate the efficiency of the produced THz radiation, as herein both models precisely follow the basic processes associated with the efficiency behavior and accurately estimate its fundamental parameters over a wide range of the applied beams intensity. In contrary, at more higher energy levels and larger quantum numbers, both models are failed to present a proper evolution for the efficiency behavior besides it is overestimated its fundamental parameters, particularly at high input beams intensity.

Acknowledgements

The author acknowledges the use of the High Performance Computing Facility at Bibliotheca Alexandrina, and the associated support services in the completion of this work.

Conflicts of Interest

The author declares no conflicts of interest regarding the publication of this paper.

References

[1] Leahy-Hoppa, M.R., Fitch, M.J., Zheng, X.Y., Hayden, L.M. and Osiander, R. (2007) Wideband Terahertz Spectroscopy of Explosives. *Chemical Physics Letters*, **434**, 227-230. https://doi.org/10.1016/j.cplett.2006.12.015

[2] Fan, S.T., Ung, B., Parrott, E.P.J. and Pickwell-MacPherson, E. (2015) Gelatin Embedding: A Novel Way to Preserve Biological Samples for Terahertz Imaging and Spectroscopy. *Physics in Medicine & Biology*, **60**, 2703-2713. https://doi.org/10.1088/0031-9155/60/7/2703

[3] Niessen, K.A., Xu, M.Y. and Markelz, A.G. (2015) Terahertz Optical Measurements of Correlated Motions with Possible Allosteric Function. *Biophysical Reviews*, **7**, 201-216. https://doi.org/10.1007/s12551-015-0168-4

[4] Ducournau, G., Szriftgiser, P., Beck, A., Bacquet, D., Pavanello, F., Peytavit, E., Zaknoune, M., Akalin, T. and Lampin, J.F. (2014) Ultrawide-Bandwidth Single-Channel 0.4-thz Wireless Link Combining Broadband Quasi-Optic Photomixer and Coherent Detection. *IEEE Transactions on Terahertz Science and Technology*, **4**, 328-337.

[5] Nagatsuma, T., Horiguchi, S., Minamikata, Y., Yoshimizu, Y., Hisatake, S., Kuwano, S., Yoshimoto, N., Terada, J. and Takahashi, H. (2013) Terahertz Wireless Communications Based on Photonics Technologies. *Optics Express*, **21**, 23736-23747. https://doi.org/10.1364/OE.21.023736

[6] Dhillon, S.S., Vitiello, M.S., Linfield, E.H., Davies, A.G., Hoffmann, M.C., Booske, J., Paoloni, C., Gensch, M., Weightman, P., Williams, G.P., Castro-Camus, E., Cumming, D.R.S., Simoens, F., Escorcia-Carranza, I., Grant, J., Lucyszyn, S., Kuwata-Gonokami, M., Konishi, K., Koch, M., Schmuttenmaer, C.A., Cocker, T.L., Huber, R., Markelz, A.G., Taylor, Z.D., Wallace, V.P., Zeitler, J.A., Sibik, J., Korter, T.M., Ellison, B., Rea, S., Goldsmith, P., Cooper, K.B., Appleby, R., Pardo, D., Huggard, P.G., Krozer, V., Shams, H., Fice, M., Renaud, C., Seeds, A., Stöhr, A., Naftaly, M., Ridler, N., Clarke, R., Cunningham, J.E. and Johnston, M.B. (2017) The 2017 Terahertz Science and Technology Roadmap. *Journal of Physics D*: *Applied Physics*, **50**, Article 043001. https://doi.org/10.1088/1361-6463/50/4/043001

[7] Grant-Jacob, G.A., Mackay, B.S., Baker, J.A.G., Xie, Y.H., McDonnell, M.D.T., Health, D.J., Praegerand, M., Eason, R.W. and Mills, B. (2019) Patterned Nanofoam Fabrication from a Variety of Materials via Femtosecond Laser Pulses. *Materials Sciences and Applications*, **10**, 186-196. https://doi.org/10.4236/msa.2019.103015

[8] Cook, D.J. and Hochstrasser, R.M. (2000) Intense Terahertz Pulses by Four-Wave Rectification in Air. *Optics Letters*, **25**, 1210-1212. https://doi.org/10.1364/OL.25.001210

[9] Kim, K.Y., Taylor, A.J., Glownia, J.H. and Rodriguez, G. (2008) Coherent Control of Terahertz Supercontinuum Generation in Ultrafast Laser—Gas Interactions. *Nature Photonics*, **2**, 605-609. https://doi.org/10.1038/nphoton.2008.153

[10] Delone, N.B. and Krainov, V.P. (1998) Tunneling and Barrier-Suppression Ionization of Atoms and Ions in a Laser Radiation Field. *Physics-Uspekhi*, **41**, 469-485. https://doi.org/10.1070/PU1998v041n05ABEH000393

[11] Ammosov, M.V., Delone, N.B. and Krainov, V.P. (1986) Tunnel Ionization of Complex Atoms and of Atomic Ions in Alternating Electromagnetic Field. *Journal of Experimental and Theoretical Physics*, **64**, 1191-1194. https://doi.org/10.1117/12.938695

[12] Tong, M., Zhao, Z.X. and Lin, C.D. (2002) Theory of Molecular Tunneling Ionization. *Physical Review A*, **66**, Article ID: 033402. https://doi.org/10.1103/PhysRevA.66.033402

[13] Walker, B., Sheehy, B., DiMauro, L.F., Agostini, P., Schafer, K.J. and Kulander, K.C. (1994) Precision Measurement of Strong Field Double Ionization of Helium. *Physical Review Letters*, **73**, 1227-1230. https://doi.org/10.1103/PhysRevLett.73.1227

[14] Litvinyuk, I.V., Lee, K.F., Dooley, P.W., Rayner, D.M., Villeneuve, D.M. and Corkum, P.B. (2003) Alignment-Dependent Strong Field Ionization of Molecules. *Physical Review Letters*, **90**, Article ID: 233003. https://doi.org/10.1103/PhysRevLett.90.233003

[15] Alnaser, A.S., Voss, S., Tong, X.M., Maharjan, C.M., Ranitovic, P., Ulrich, B., Osipov, T., Shan, B., Chang, Z. and Cocke, C.L. (2004) Effects of Molecular Structure on Ion Disintegration Patterns in Ionization of O_2 and O_2 by Short Laser Pulses. *Physical Review Letters*, **93**, Article ID: 113003.

[16] Chen, Y.Q., Yamaguchi, M., Wang, M.F. and Zhang, X.C. (2007) Terahertz Pulse Generation from Noble Gases. *Applied Physics Letters*, **91**, Article ID: 251116. https://doi.org/10.1063/1.2826544

[17] Rodriguez, G. and Dakovski, G.L. (2010) Scaling Behavior of Ultrafast Two-Color Terahertz Generation in Plasma Gas Targets: Energy and Pressure Dependence. *Optics Express*, **18**, 15130-15143. https://doi.org/10.1364/OE.18.015130

[18] Debayle, A., Gremillet, L., Bergé, L. and Kohler, C. (2014) Analytical Model for THz Emissions Induced by Laser-Gas Interaction. *Optics Express*, **22**, 13691-13709. https://doi.org/10.1364/OE.22.013691

[19] Chen, W.B., Huang, Y.D., Meng, C., Liu, J.L., Zhou, Z.Y., Zhang, D.W., Yuan, J.M. and Zhao, Z.X. (2015) Theoretical Study of Terahertz Generation from Atoms and Aligned Molecules Driven by Two-Color Laser Fields. *Physical Review A*, **92**, Article ID: 033410. https://doi.org/10.1103/PhysRevA.92.033410

[20] Johnson, K., Price-Gallagher, M., Mamer, O., Lesimple, A., Fletcher, C., Chen, Y.Q., Lu, X.F., Yamaguchi, M. and Zhang, X.C. (2008) Water Vapor: An Extraordinary Terahertz Wave Source under Optical Excitation. *Physics Letters A*, **372**, 6037-6040. https://doi.org/10.1016/j.physleta.2008.07.071

[21] You, Y.S., Oh, T.I., Fallahkhair, A.B. and Kim, K.Y. (2013) Alignment-Dependent Terahertz Radiation in Two-Color Photoionization of Molecules. *Physics Letters A*, **87**, Article ID: 035401. https://doi.org/10.1103/PhysRevA.87.035401

[22] Moradi, S., Ganjovi, A., Shojaei, F. and Saeed, M. (2015) Parametric Study of Broadband Terahertz Radiation Generation Based on Interaction of Two-Color Ultra-Short Laser Pulses. *Physics of Plasmas*, **22**, Article ID: 043108. https://doi.org/10.1063/1.4916123

[23] Bauer, D. and Mulser, P. (1999) Exact Field Ionization Rates in the Barrier-Suppression Regime from Numerical Time-Dependent Schrödinger-Equation Calculations. *Physical Review A*, **59**, 569-577. https://doi.org/10.1103/PhysRevA.59.569

[24] Tong, X.M. and Lin, C.D. (2005) Empirical Formula for Static Field Ionization Rates of Atoms and Molecules by Lasers in the Barrier-Suppression Regime. *Journal of Physics B: Atomic, Molecular and Optical Physics*, **38**, 2593-2600. https://doi.org/10.1088/0953-4075/38/15/001

[25] Scrinzi, A., Geissler, M. and Brabec, T. (1999) Ionization above the Coulomb Barrier. *Physical Review Letters*, **83**, 706-709. https://doi.org/10.1103/PhysRevLett.83.706

[26] Soltani Gishini, M.S. and Ganjovi, A. (2017) Thz Radiation Generation via the Interaction of Two-Colour Ultra-Short Laser Pulses with SO_2 and NH_3 Gases. *Contributions to Plasma Physics*, **57**, 293-310. https://doi.org/10.1002/ctpp.201700018

[27] Sissay, A., Abanador, P., Mauger, F., Gaarde, M., Schafer, K.J. and Lopata, K. (2016) Angle-Dependent Strong-Field Molecular Ionization Rates with Tuned Range-Separated Time-Dependent Density Functional Theory. *The Journal of Chemical Phys-*

ics, **145**, Article ID: 094105. https://doi.org/10.1063/1.4961731

[28] Wang, R., Zhang, Q.B., Li, D., Xu, S.L., Cao, P.K., Zhou, Y.M., Cao, W. and Lu, P. (2019) Identification of Tunneling and Multiphoton Ionization in Intermediate Keldysh Parameter Regime. *Optics Express*, **27**, 6471-6482. https://doi.org/10.1364/OE.27.006471

[29] Kjeldsen, T.K. and Madsen, L.B. (2004) Strong-Field Ionization of N_2: Length and Velocity Gauge Strong-Field Approximation and Tunnelling Theory. *Journal of Physics B*: *Atomic*, *Molecular and Optical Physics*, **37**, 2033-2044. https://doi.org/10.1088/0953-4075/37/10/003

[30] Yee, K. (1966) Numerical Solution of Initial Boundary Value Problems Involving Maxwell's Equations in Isotropic Media. *IEEE Transactions on Antennas and Propagation*, **14**, 302-307. https://doi.org/10.1109/TAP.1966.1138693

[31] Guo, C., Li, M., Nibarger, J.P. and Gibson, G.N. (1998) Single and Double Ionization of Diatomic Molecules in Strong Laser Fields. *Physical Review A*, **58**, R4271-R4274. https://doi.org/10.1103/PhysRevA.58.R4271

[32] Guo, H.C., Du, H.L. and Liu, C.P. (2022) Theoretical Investigation of THz Radiation Generation from Air-Plasma Based on an Improved FDTD Algorithm. *Proceedings of the SPIE*, **12291**, Article ID: 1229109.

[33] Tarchoun, B., El Ouafi, A. and Chebak, A. (2020) Numerical Investigation of Laser Surface Hardening of AISI 4340 Using 3D FEM Model for Thermal Analysis of Different Laser Scanning Patterns. *Modeling and Numerical Simulation of Material Science*, **10**, 31-54. https://doi.org/10.4236/mnsms.2020.103003

[34] Kim, K.Y., Glownia, J.H., Taylor, A.J. and Rodriguez, G. (2007) Terahertz Emission from Ultrafast Ionizing Air in Symmetry-Broken Laser Fields. *Optics Express*, **15**, 4577-4584. https://doi.org/10.1364/OE.15.004577

[35] Hussien, A.M.M. (2015) Ionization of Diatomic Molecules in Intense Laser Fields. Ph.D. Thesis, Humboldt-Universität zu Berlin, Berlin.